Biocompatible features of magnetic nano-oxide core/ PCL shell 3D composites fabricated via SLS/M process

Igor Shishkovsky [1-2], Stanislav Volchkov[2], Vladimir Scherbakov[1], Larisa Volova[2]**

[1]*P.N. Lebedev Physic Institute of RAS, Samara Branch, Novo-Sadovaja st., Samara, 443011, Russia*
[2]*Samara State Medical University, Chapaevskaja St., Samara, 443096, Russia*

DOI: 10.5185/amlett.2018.1676
www.vbripress.com/aml

Abstract

Superparamagnetic oxide nanoparticles attract increasing attention in biomedical applications for tagging, imaging, separation and/or purification of cancer cells in living tissue. At the present study the selective laser sintering/melting (SLS/M) process using the Nd^{+3}YAG laser was carried out to fabricate and characterize polymer composites based on nano-oxides of Fe_xO_y type or of high-temperature superconductivity (HTS) of $SrFe_{12}O_{19}$ with bioresorbable polycaprolactone (PCL) powders and manufacture porous tissue engineering scaffolds. Practicability of the method for synthesis of functional-gradient three dimensional (3D) parts with magnetic nano-oxide particles and structural ordering were shown and appropriated laser regimes were assigned. The stem cellular morphometry, proliferative and adhesive activity to the 3D magnetic nanocomposites were compared. The medical tests show that all the 3D printed composites have biocompatible features. Medical potential of the SLS/M-fabricated superparamagnetic nano oxides for application as cell targeting systems and tissue engineering scaffolds is being discussed. Copyright © 2018 VBRI Press.

Keywords: selective laser sintering/melting (SLS/M), superparamagnetic oxides, high-temperature superconductivity (HTS), functional gradient nanocomposites, polycaprolactone (PCL), multipotent mesenchymal stem cells (MMSC), scaffolds.

Introduction

Superparamagnetic nano-oxide particles seem perspective for manufacturing of drug delivery systems and tissue engineering scaffolds [**1-5**]. Nanoparticles with magnetic properties can be included into biodegradable polymer matrix to provide reverberative response to alternating external magnetic field of special amplitude and frequency, and simultaneously effective absorption of electromagnetic energy and its transferring into heating of surrounding living tissues. Actually, a magnetic nanoparticle in electromagnetic field can be applied as hyperthermia instrument to deliver lethal quantity of energy to the cells of tumor [**6**]; or for additional facilitation during chemotherapy or laser therapy, where magnetic nano-oxide particles provide reasonable heating so that destruction of the cancerous tissue becomes more effective. The particles aiming to be applied for magnetic hyperthermia should have high SAR (specific absorption rate), which allows their quick heating in variable magnetic field. Typical tumor cells do not survive the temperature above 42...43 degrees.

One of promising spheres for medical application of magnetic nanoparticles is vector drug delivery [**6**]. But all the possible applications: targeted drug delivering systems, separation of physiologically active substances, diagnostic magnetic markers, controllable hyperthermia, - demand new approaches, ensuring a reproducibility of receiving the most important magnetic nano-oxide characteristics.

A wide spectrum of materials is now being tested as potential choices for magnetic hyperthermia: maghemite (γ-Fe_2O_3) and magnetite (Fe_3O_4) - still ferrimagnetic iron oxides, or high temperature superconductor (HTS) of $SrFe_{12}O_{19}$ [**5, 8**]. These materials are more oxidation-resistant than metal nanoparticles; have higher magnetization; are less disposed to induce oxidative stress toxicity in vivo; their metabolism is quite well known, and they are approved for use in humans by Food and Drug Administration.

It seems possible to resolve this problem by isolating the nanoparticles into inert materials, where aggregation and "aging" will not happen, but they can still be controllably released with retained biochemical and phase-structural composition. The aim was to project and develop nanocomposite substrates with magnetic properties and being fully biodegradable for engineering of bone tissue. The substrates consisted of polycaprolactone (PCL) matrices hardened with biodegradable iron-doped hydroxyapatite (Fe-HA) nanoparticles [**9**]. The proposal of developing magnetic scaffolds to manage angiogenesis *in vivo* was studied by N.Bock et al. [**10**], where magnetic samples were fabricated by enamel coating of scaffolds in aqueous ferromagnetic containing FexOe nano-oxide particles covered with special polymers of some biochemical function.

The selective laser sintering/melting (SLS/M) as one of methods the powder bed fusion for conservation of

magnetic particles is promising for fabricating functional systems for medicine and gradient structures with nano-sized inclusions [7—10]. But it is quite difficult technologically to fabricate the scaffolds from nano powders by multilayered techniques directly. It is well known, that sintering is a thermally stimulated process, and meanwhile nanoparticles coagulate into micro-sized conglomerates. Nevertheless, there is experience of developing 3D nanocomposite PCL/ Fe-HA matrices with useful magnetic features and peculiar structure in [**11**] using a bio-inkjet printer system. To settle the needed nanoparticle's distribution over the polymer, which protects the particles from corrosion and oxidation and also to get functionally graded (FG) structures, stabilization of the nanoparticles in polymer matrices and additional reinforcement of porous structure can be used [**12, 13**]. Also, the polymer can be applied to cover the magnetic particles and enhance their blood circulation period by helping them to evade reticuloendothelial system [**1**]. The results represent that nanoparticles reinforce the polymer matrices mechanically; the modulus of elasticity and the maximum strain-stress increase by about 10% and 30%, correspondingly [**14**]. But the maximum deformation decreases by ~ 50%; which gives evidence of enhanced brittleness.

In the work [**15**] we showed how a powder bed fusion approach of 3D biosynthesis was applied to fabricate a porous polyetheretherketone (PEEK) shell structures including encapsulated of nano-oxide Al_2O_3, ZrO_2, AZO, TiO_2 and hydroxyapatite particles, which were heterogeneously distributed by the matrix of the SL-Sintered polymer.

At the present study properties of the superparamagnetic nanooxide particles were examined before the experiment. The SLS process was applied to fabricate and characterize the hardened nanopolymer composite based on nano oxides of Fe_xO_y type or HTS of $SrFe_{12}O_{19}$ with bioresorbable polycaprolactone (PCL) powder and to manufacture magnetic oxide core/ porous PCL shell vectoring systems.

Materials and experimental procedure

Materials preparation

The object of the study was bioresorbable polycaprolactone (PCL – Polymorph Co., UK). The polymeric fraction particles had size of 70 μm, comparable with the diameter of laser spot. The Fe/Fe_xO_y aerosol nanoparticles or the HTS $SrFe_{12}O_{19}$, prepared at the Russian Institute of Structural Macrokinetics and Material Sciences (ISMMS) [**8, 16**], were used as a filling material. The mean size value of Fe_xO_y particles were from 42 to 235 nm. **Table S1** shows the key particular parameters of the sintered nanoparticles F02-F07 series: density - ρ (column 3); X-ray diffraction (XRD) phase-structural composition (column 4); and specific surface area - *S* (column 5) depending on the average particle sizes *d* (column 2). The HTS had near submicron sized particles (~ 2 - 4 μm). Polymeric nanocomposites were set for the SL-Sintering process in the following ratios by weight: 1:10, 1:100 (the first proportion is for the NPs).

A cw YAG:Nd^{+3} laser was carried out to perform the SLS/M process. The laser beam power - *P* changed between 2 and 8 W. The laser ray scanned the surface of the powder bed mixture; the hatching distance between laser ray passages (70 μm) did not significantly differ from the diameter of laser beam. The optical equipment had a focal length of 147 mm and a 25-mm shift from the bottleneck. The SL-Sintering process was carried out in an original designed chamber under argon or air environment as it is described before [**16, 17**].

As an outcome of laser-assisted fabrication for medical preclinical tests both plain porous 2D samples of matrices sized ~ 10 × 10 × d mm, where d - is a monolayer thickness (~ 0.5-1 mm depending on the laser regime, fig. 1 a) and three dimensional (3D) samples were obtained (**Fig. 1 b-c**). Gradient sample (**Fig. 1c**) was obtained account of alternation PCL+FO3 mixture - through each 5 layers, the mixture composition was changing from pure PCL on the bottom to 1:10 and 1:100 ratio FO3+PCL in middle and top layers. White color – PEEK; grey color – the HTS inclusions. The samples of the type (**Fig. 1a**) were used in the following medical tests.

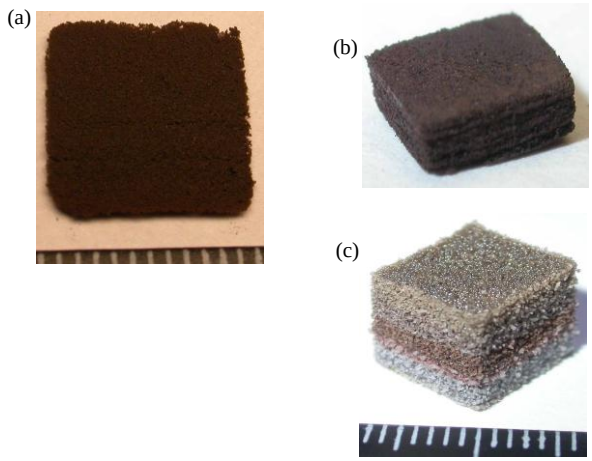

Fig. 1. The SLS of the 2D monolayer of PCL+FO2 (a), 3D samples PCL+ $SrFe_{12}O_{19}$ (b) and functional graded PCL+FO3 (c) with magnetic nano inclusions. All the 2D and 3D samples have area of surface ~ 10x10 mm^2.

Stem cell culture preparation and treatment

The design of the experiment included three parts of the works carried out. The first one was preparing the materials for the research, the second one – testing their toxicity in separated cameras, and the third one – cultivating the multipotent mesenchymal stem cells (MMSC) on the substrate.

Pure growth mediums with stem cells without samples and with biocompatible PCL sample were used as a control group (reference group). All the samples from polymer + nanoparticles inserted into the growth medium with stem cells were considered as testing groups. All the

3D bioprinted samples were first washed in a sterile phosphate salt buffer (PBS) by reiterated immersion and active stirring of the samples in the solution. After that the samples were sterilized in a Steridент steam sterilizer at the temperature of 121^0C and pressure of 120 κPa for 20 min. The third passage MMSC was chosen. The cells were taken from umbilical cord of an adult donor, who preliminarily subscribed an informed consent to donate the biomedical material in agreement with the international legislation. Isolation of the cells was accomplished on the Ficcol consistence gradient 1.033. The cell inoculation on the material was carried out in a new 6 cavities plotter. The materials under investigation were brought into the clean cavities, then MMSC with concentration of 100 thousand cells per 1 cm^2 and maximal volume of 500mcl of the growth medium were applied right upon them. Then the material was incubated for 3 hours to ensure the adhesion of the cells to the material (the preliminary incubation).

Cultivation lasted 7 days using standard nutrient mediums including aMEM (Sigma), 2mM alanil-glutamine (Invitrogen Co.) and 10% selected calf serum (Gibco Co.) by design scheme. We were changing the nutrient medium every 4 days or every time we indicated the medium pH alteration had changed.

For every group daily morphometry was carried out. The cell-covered area was estimated using Axio ObserverA1 microscope and software package produced by Carl Zeiss in Axio Vision Inc. The culture cluster analysis was conducted on the ImageJ and Image ProPlus bundled software, and the cells were divided into groups in accordance with their pixel density per object. The immunophenotyping procedure was accomplished on a running FACS Canto (Becton Dickinson Co.) cytofluorometer right before inoculation and after removal of the stem cells on the 0^{th} and 7^{th} day of cultivation. We studied the following antigens: CD73+, CD 90+, CD 105+, CD 34-, CD 45.

The cells were counted and their proliferate activity estimated for all the experimental groups by bundled Vi-Cell XR software made by Becman Coulter, before inoculation and after the cultivation finished. The activity of proliferation was counted in accordance with the equation: $X = [\log10(N_H) - \log10(N_I)]/\log10(2)$, where N_H is cell's number by the time of inoculation, N_1 – the accretion of the cells quantity. The data on the number of duplications in the culture during the cultivation was obtained using this formula. The speed of reduplication (i.e. duplications per hour) is convenient to be counted during the certain quantity of duplications, applying the following equation: $X = C_t/D_t$, where C_t is cultivation time (an hour), D_t – quantity of the culture duplications. The statistical data processing was carried out with use of the Student's t-criterion with all the values of $p<0,05$ considering significant.

The cells on the materials were estimated through fluorescent microscopy on Axiovision A1 (Carl Zeiss, Germany) microscope using fluorescent coloring agents DAPI (Life Technologies, USA) and WGA (Wheat Germ Agglutinin Sampler Kit) (ThermoFisher, USA). The nuclei were colored blue by DAPI coloring agent and the cell structures were colored red by WGA. Colouring was carried out at the last stage of the experiment. Estimation of cell presence in 2D & 3D matrices at ultrahigh magnifications was carried out on a SEM JEOL JSM-6390 after sample preparation. Essence of the sample preparation was fixing the cells with 0.4% solution of formalin during 15 minutes, then dehydrating in rising concentrations of 10% ethanol solution and then evaporation on a JEOL add-on of XeDraw-BLANK. Estimation of material loss (biodegradation) was carried out through weighting the materials on ultra precision balance OHAUS Explorer Pro (New Jersey, USA) before and after the experiment. Spectral characteristics of the samples were studied on an experimental stand including a high resolution digital spectrometer Shamrock Sr-303i with a built-in cooling camera Andor DV420A-OE, fiber optic probe for Raman scattering (RS) spectroscopy RPB785 united with laser setup Luxx Master LML-785.0RB-04 of 500 mW power and 785 nm wavelength.

Results and discussion

Fig. 2 and **Table 1** show results of RS spectroscopy in PCL+ FexOy matrices and description of the main peaks. The investigations prove that we deal with PCL with ferric oxides inclusions.

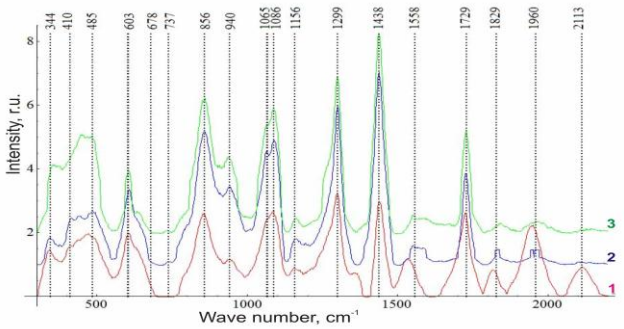

Fig. 2. Average CS spectrum of 2D samples: (1) PCL+FO2; (2) PCL+FO3; 3) PCL+FO4.

Table 1. Wave number properties of 2D samples by **Fig. 2.**

Wave number, cm^{-1}	Oscillation	Materials
603		Fe-O vibration
856-859	ν (C–COO)	C-C extension
938 - 940	C-C-O	CH
1062-1065	C-O-O	C-C extension
1086-1087	ν_s(C–O–C)	C-O single linkage from ether links in PCL
1156-1057	ν (C-O-C)	C-O and C-C extension in amorphous phase
1299-1301	ωCH_2	CH_2
1438 -1440	δCH_2	CH_2
1726-1729	νC=O	ketonic groups of PCLs

Optic microscopy and morphology of the structures is depicted schematically in **Fig. S1** (top line) for the 3rd day and in **Table S2** for the 6th. **Fig. S1** also represents a typical morphology of MMSC next to the matrix for the main types of the matrices (the upper row). So, we can see that culture density near the PCL+FO3 was 50% on the 3rd day, the cells had fibroblast-like morphology and were actively dividing. But the samples with FO4 and FO7 had culture density of only 30%, and only 15% for the one with FO6. Near the ones with FO6 – FO7 cells in apoptosis were found. Near the PCL + $SrFe_{12}O_{19}$ matrix culture density was 40%, morphology and activity of the cells were the same as near the FO3 matrix. Near the PCL only sample culture had density of 20%, the cells had fibroblast-like morphology, and their divisions were observed as well as apoptosis. So by the 6th day we mentioned:

- The level of confluence in the reference groups was of about 80-90% which stands for a monolayer;
- The same growth was observed in cavities numbered 1, 2, 3, 4, 5, 6 (see **Table S2**). Culture density here also went up to 80-90% and achieved the level of a monolayer;
- In all the other cavities density of about 60-70% was observed;
- Cell morphology is uniform, fibroblast-like without stress-fibers in all the cavities;

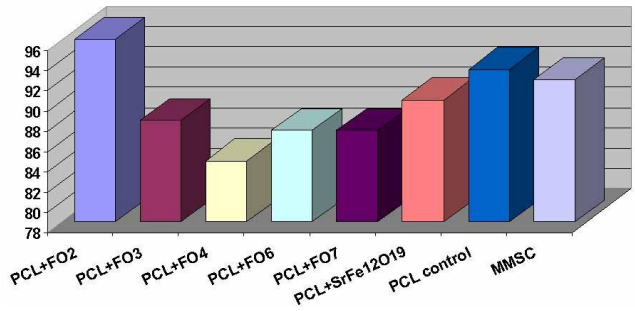

Fig. 4. Stem cell viability (%) on the 6th day.

Proliferative activity and viability of the cells are shown in **Figs. 4-5**. In comparison with the reference group sample (MMSC and PCL only) these parameters of crucial importance meet out expectations and even exceed them for some samples.

Results of estimation of MMSC ability to adhere to 2D matrices and divide on them are shown in **Fig. S1** (middle row). The materials with cells on them were colored with nuclear DAPI coloring agent (Life Technologies, USA) and estimated by presence of fluorescence in a confocal microscope with wavelength of 420 nm. So it is seen that there are many nuclei (blue fluorescence on different levels) near PCL+FO3 in the field of vision, which can testify for cells growing into the material. Near PCL + $SrFe_{12}O_{19}$ few nuclei are visible in the field on the growing background. Then, near PCL only there are many nuclei in the field situated on different levels which stands for significant growth of the cells into the material.

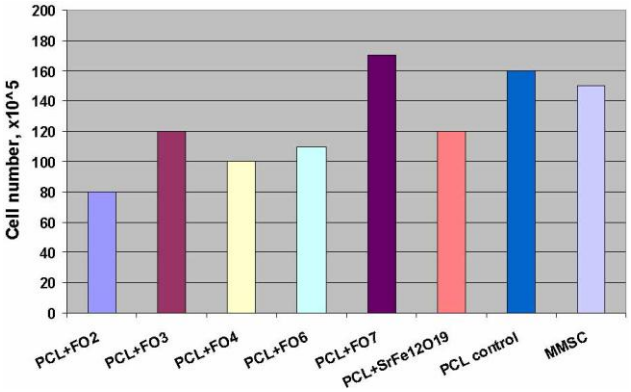

Fig. 5. Stem cell culture density on the 6th day.

After the medical test an estimation of MMSC on the materials was carried out using SEM with great magnification (**Fig. S1** - third row). In the case of FO3 matrix we observe some large groups of the cells in monolayer form. 2D samples with FO2, FO4, FO7 and $SrFe_{12}O_{19}$ had no such groups. But 2D samples with FO6 and pure PCL had traces of cells bioactivity in many areas (see **Fig. S1** - third line). So SEM visualization of MMSC shows that groups of stems cells undoubtedly fix to samples 2 and 7 (**Table S2**). All the other materials had no evident signs of cell fixation. Such a result can come from the material properties (great adhesive ability), but also with harshness of sample preparation procedure (the cells could have been washed away). L. Gutierrez *et al.* [**18**] denoted that the magnetic core/shell types, sizes, values between them, and their redistribution over the matrices – everything will significantly influence the magnetic features of the synthesized objects and prospective medical properties.

Conclusion

We demonstrated principal practicability of the method for manufacturing of functional gradient 3D samples with FexOy nano-oxide particle structural ordering and determined appropriated SLS/M regimes.

Biocompatibility of the materials presented was estimated. We considered biocompatible the materials with no negative influence on cells, the ones easy for MMSC to adhere on their surface and grow into. The following samples sintered by 3D printing meet these requirements:

- PCL + FO2- with nanoparticles ~ 235 nm (60% nano magnetite Fe_3O_4 and 30 % hematite –Fe_2O_3, bal. Fe);
- PCL + FO3- with nanoparticles ~ 135 nm (35% nano magnetite Fe_3O_4 and 50 % hematite –Fe_2O_3, bal. Fe);
- PCL + FO4- with nanoparticles ~ 113 nm (95 % hematite –Fe_2O_3, bal. Fe);
- PCL + FO7- with nanoparticles ~ 42 nm (100 % hematite –Fe_2O_3);
- pure PCL (control sample).

The SLS-fabricated 2D and 3D samples of magnetic oxide core and bioresorbable PCL shell nanocomposites are perspective for application in medicine for cell targeting systems and tissue engineering scaffolds.

Acknowledgements

The study was supported by the Russian Science Foundation (project n. 15-19-00208). Authors thank Prof. Yu. Morozov (ISMAN RAS) for presentation and evaluation of nano iron powders.

Author's contributions

Conceived the plan: Igor Shishkovsky, Vladimir Sherbakov, Stanislav Volchkov; Performed the expeirments: Vladimir Scherbakov, Stanislav Volchkov; Data analysis: Igor Shishkovsky, Larisa Volova; Wrote the paper: Igor Shishkovsky. Authors have no competing financial interests.

References

1. Kumar, A.; Jena, P.K.; Behera, S.; Lockey, R.F.; Mohapatra, S.; *Nanomedicine: Nanotechnology, Biology, and Medicine*, **2010,** *6*, 64. **DOI:** 10.1016/j.nano.2009.04.002
2. Qiang, Y.; Antony, J.; Sharma, A.; Nutting, J.; Sikes, D.; Meyer, D.; *J. of Nanoparticle Res.*, **2006**, *8*, 489. **DOI:** 10.1007/s11051-005-9011-3
3. Leostean, C.; Pana, O.; Turcu, R.; Soran, M.L.; Macavei, S.; Chauvet, O.; Payen. C.; *J. of Nanoparticle Res.*, **2011**, *13*, 6181. **DOI:** 10.1007/s11051-011-0313-3
4. Riegler, J.; Liew, A; Hynes, S.O.; Ortega, D.; O'Brien, T.; Day, R.M.; Richards, T.; Sharif, F.; Pankhurst, Q.A.; Lythgoe, M.F.; *Biomaterials*, **2013**, *34*, 1987. **DOI:** 10.1016/j.biomaterials.2012.11.040
5. Ortega, D; Pankhurst, Q.A.; Magnetic hyperthermia, In Nanoscience: Volume 1: Nanostructures through Chemistry, O'Brien, P.; (Ed); Royal Society of Chemistry: Cambridge, UK, **2013**, pp. 60-88. **DOI:** 10.1039/9781849734844-00060
6. Volyansky, I.; Shishkovsky, I.; Laser assisted 3D printing of functional graded structures from polymer covered nanocomposites. In New Trends in 3D Printing, Shishkovsky I. (Ed.); InTech Publ. Croatia, **2016,** pp. 237-258. **DOI:** 10.5772/63565
7. Blanco-Andujar, C.; Ortega, D.; Southern, P.; Pankhurst, Q.A. ; Thanh, N.T.K.; *Nanoslace*, **2015**, 7, 1768. **DOI:** 10.1039/c4nr06239f
8. Shishkovsky, I.; Sherbakov, V.; Morozov, Yu.; *Microelectronic Engineering*, **2015**, *146*, 85. **DOI:** 10.1016/j.mee.2015.04.030
9. Gloria, A; Russo, T.; D'Amora, U.; Zeppetelli, S.; D'Alessandro, T.; Sandri, M.; Lorpez, M.B.; Redondo, Y.P.; Uhlarz, M.; Tampieri, A.; Rivas, J.; Erfer, T.H.; Dediu, V.A.; Ambrosio, L.; De Santis, R.; *J. R. Soc. Interface*, **2013**, *10*, 20120833. **DOI:** 10.1098/rsif.2012.0833
10. Bock, N.; Riminucci, A.; Dionigi, C.; Russo, A.; Tampieri, A.; Landi, E.; Goranov, V.A.; Marcacci, M; Dediu, V; *Acta Biomater.*, **2010**, *6*, 786. **DOI:** 10.1016/j.actbio.2009.09.017
11. Russo, T.; D'Amora, U.; Gloria, A.; Tunesi, M.; Sandri, M.; Rodilossi, S.; Albani, D.; Forloni, G.; Giordano, C.; Cigada, A.; Tampieri, A.; De Santis, R.; Ambrosio, L; *Procedia Engineering*, **2013**, *59*, 233. **DOI:** 10.1016/j.proeng.2013.05.116
12. Hu, H.; Xu, G., Zan, Q.; Liu, J.; Liu, R.; Shen, Z.; Ye, X.; *Microelectron. Eng.*, **2012**, *98*, 566. **DOI:** 10.1016/j.mee.2012.07.001
13. Shishkovsky, I.V.; Morozov, Yu.G.; *J. of Nanoscience and Nanotechnology*, **2013**, *13/2*, 1440. **DOI:** 10.1166/jnn.2013.6010
14. De Santis, R.; Gloria, A.; Russo, T.; D'Amora, U.; Zeppetelli, S.; Dionigi, C.; Sytcheva, A.; Herrmannsdörfer, T.; Dediu, V.; Ambrosio, L; J. of Applied Polymer Science, **2011**, *122*, 3599. **DOI:** 10.1002/app.34771
15. Shishkovsky, I.; Nagulin, K.; Sherbakov, V.; *Inter. J. of Adv. Manufacturing Tech.*, **2015,** *78*, 449. . **DOI:** 10.1007/s00170-014-6633-6
16. Shishkovsky, I.; Scherbakov, V.; Kuznetsov, M.; *Opt. and Quantum Electronics*, **2016**, *48(10)*, 487. **DOI:** 10.1007/s11082-016-0755-z
17. Shishkovskii, I.V.; Morozov, Yu.G.; Fokeev, S.V.; Volova, L.T.; *Powder Metallurgy and Metal Ceramics*, **2012**, *50(9/10)*, 606. **DOI:** 10.1007/ s11106-012-9366-9
18. Gutiérrez, L.; Costo, R.; Grüttner, C.; Westphal, F.; Gehrke, N.; Heinke, D.; Fornara, A.; Pankhurst, Q.A.; Johansson, C.; Veintemillas-Verdaguer, S.; Morales ,M.P; *Dalton Transactions*, **DOI:** 10.1039/c4dt03013c

